

Towards the Semantic Weak Generalization Problem in Generative Zero-Shot Learning: Ante-hoc and Post-hoc

Dubing Chen^{1*}, Yuming Shen^{2*}, Haofeng Zhang^{1✉}, and Philip H.S. Torr²

¹ Nanjing University of Science and Technology
{db.chen, zhanghf}@njust.edu.cn

² University of Oxford
ym_zmxncbv@hotmail.com, philip.torr@eng.ox.ac.uk

Abstract. In this paper, we present a simple and effective strategy lowering the previously unexplored factors that limit the performance ceiling of generative Zero-Shot Learning (ZSL). We begin by formally defining semantic generalization, then look into approaches for reducing the semantic weak generalization problem and minimizing its negative influence on classifier training. In the ante-hoc phase, we augment the generator’s semantic input, as well as relax the fitting target of the generator. In the post-hoc phase (after generating simulated unseen samples), we derive from the gradient of the loss function to minimize the gradient increment on seen classifier weights carried by biased unseen distribution, which tends to cause misleading on intra-seen class decision boundaries. Without complicated designs, our approach hit the essential problem and significantly outperform the state-of-the-art on four widely used ZSL datasets.

Keywords: Generative Zero-Shot Learning, Semantic Weak Generalization

1 Introduction

With the enormous expansion of picture classes, there is a growing requirement for computer vision systems to recognize images from previously unseen classes, a challenge known as Zero-Shot Learning (ZSL) [33]. In general, ZSL seeks to recognize unseen data by exploiting correlations between seen and unseen data. This relation mining is based on prior semantic knowledge, which is manually annotated [24] or captured by word-to-vector [31]. Through the semantic descriptors, ZSL allows information transfer from seen to unseen domains. Recently, more researchers pay their attention to the more realistic GZSL settings, whose target decision domain contains additional seen classes compared to ZSL.

A family of GZSL methods adopts generative models to simulate the unseen samples, which refocuses a part of the focus from zero-shot classification

* Equal contribution.

✉ Corresponding author.

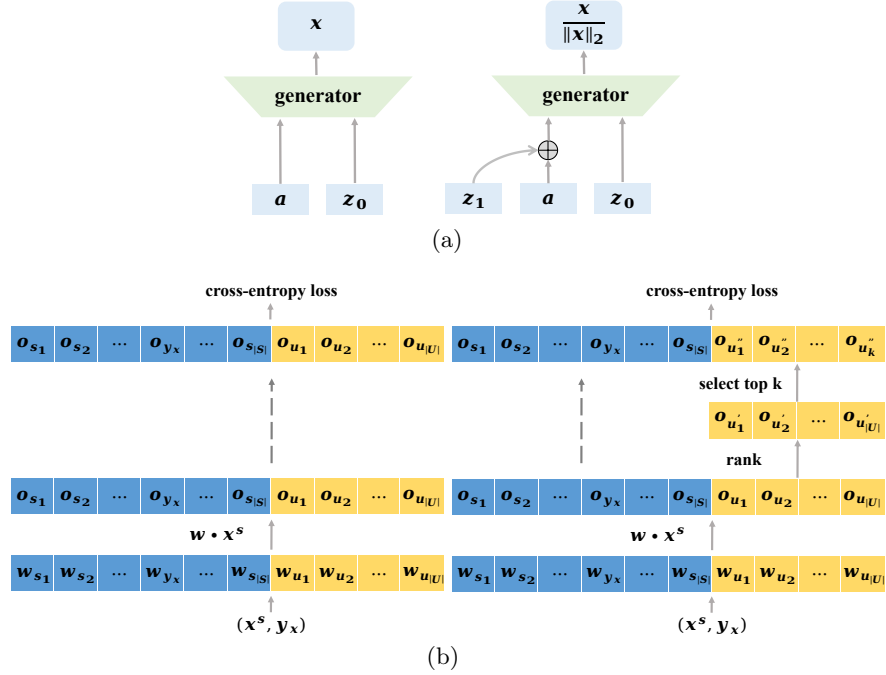


Fig. 1: Conceptual comparison of our revision, we plot our revision version on the right of two subfigures, compared to the original form on the left. **(a) Ante-hoc process:** we augment the generator’s semantic input with Gaussian noise, and change its fitting target. **(b) Post-hoc process:** we select top k unseen logits (o_u) meeting a **seen datum** and drop the rest, where \mathbf{W} is the classifier weights, and the subscript indicates the weight of the corresponding class (s and u denote seen and unseen classes, respectively).

to zero-shot generation. Although the generative-based method achieves good ZSL performance, and the classifier trained on the original image can accurately identify the seen class effectively, the prediction accuracy of both the unseen and seen classes reduces substantially as the classification domain expands. As the attention on ZSL grows, new solutions are being presented. However, the phenomenon of seen-unseen bias (i.e. easily classify unseen class samples to seen classes) persists, and the GZSL results with the generative-based methods are still unsatisfactory. Regardless of the traditional ZSL challenges, such as the domain shift and the hubness problem, we pose the following question: textitwhat limits the performance ceiling of generative-based methods? We attempt to answer this question from the following perspectives:

(i) Until recently, generator modeling does not take into account the problem of semantic generalization. The task of zero-shot generators is different from ordinary conditional generators, i.e., zero-shot generators need to be trained on seen classes and generate sufficiently realistic unseen class samples. However, zero-shot generators are usually trained as ordinary conditional generators, ignoring

the generalization problem on unseen class semantics. An obvious inconsistency can be observed between the generated and real unseen distributions, as shown in Fig. 3.

(ii) Existing approaches do not differentiate between biased and unbiased data in the classifier learning phase. Generally, there is no distinction between real and biased data in classifier optimization. As a result, the classifier matches the class boundaries between the seen and biased unseen classes, as well as the class boundaries between distinct biased unseen classes, and thus is unable to prevent the adverse impact of biased unseen data on the seen class decision boundaries.

Driven by this analysis, we first formally define the semantic generalization problem, then conduct an empirical study on the bound of generalization. To improve semantic generalization and efficiently optimize the classifier with partially biased data, we launch our research ante-hoc and post-hoc the generator training phase. We consequentially augment the generator’s semantic input and relax its fitting target to enhance its semantic generalization ability (Fig. 1 (a), (b)). After generating simulated unseen samples, we establish two concepts to guide the correct optimization direction of the classifier, i.e., limiting the misleading to the decision boundary between different seen classes induced by the biased distribution, and lowering the seen-unseen bias. We finally reduce the number of unseen class weights in the loss function corresponding to the seen class points according to the concepts, as shown in Fig. 1 (c), (d). Our main contributions include:

- We formally define semantic generalization in generative ZSL, which will serve as a guideline for future development.
- We propose to enhance semantic generalization by semantic augmentation and fitting target relaxation in generator training.
- In classifier training, we derive to minimize the gradient increment created by the unseen class weights in the loss function when facing a seen class datum.
- Without complicated design on the framework, the proposed method achieves SoTAs on four popular ZSL benches.

2 Related Work

Zero-Shot Learning. ZSL [24,9] has been extensively studied in recent years. Traditional ZSL models [1,11] typically learn a semantic-visual projection between visual instances and their corresponding semantics, which are effective in ZSL but has slightly effect in the more challenging Generalized Zero-Shot Learning (GZSL) [3,45] settings. In the context of deep learning, the recent advent of generative models [13,23] delves deeper into the semantic-visual relation by incorporating it into the generative paradigm, allowing the generation of simulated unseen samples via the relation transfer on semantics. Furthermore, other schools of ZSL methods have emerged with the development of deep learning.

Attention based methods [50,20,47], meta-learning based methods [41,48], contrastive learning based methods [21,16], etc. promote the development of ZSL from different aspects.

Problems in ZSL. In ZSL, the presentation of key problems directs the design of approaches. The domain shift problem [12] concerns the different visual representations of the same attribute. The hubness problem [8] considers that some points become the nearest neighbors of most points in high-dimensional spaces. Semantic gap problem [28] focuses on the inconsistency between the manifold in the visual space and semantic space. We present the semantic generalization problem in this paper, and we investigate ante-hoc and post-hoc solutions based on this challenge.

Recent Development in Generative ZSL. As one of the mainstream directions in ZSL, various researches have been conducted to improve the performance of generative ZSL. [46,36] focus their attention on new generative frameworks. [41] explores the training method. These methods do not make full use of the prior information in the ZSL setting, but seek breakthroughs from other fields. [10] utilizes semantics for secondary supervision during generator training. [32] design a recurrent structure that utilizes the intermediate layers of the visual-to-semantic mapping network for secondary generation. [17,16,6] propose to transform the real and generated visual feature to a semantically relevant latent space. These approaches either strengthen the semantic factors in the generated visual features [10,32] or add semantic factors to the discriminative process [17,16,6], all ignoring the difference between zero-shot generation tasks and ordinary conditional generation tasks, i.e., the problem of semantic generalization. Meanwhile, most of the above methods rely on complex designs and require high time complexity. In this work, we study towards semantic generalization, and give a solution closer to the essence of the problem, which can achieve SoTA without complex design.

3 Methodology

Assume there are two disjoint class label sets \mathcal{Y}^s and \mathcal{Y}^u , ZSL aims at recognizing samples belong to \mathcal{Y}^u while only access to samples with the labels in \mathcal{Y}^s during training. Denote $\mathcal{X} \subseteq \mathbb{R}^{d_x}$ and $\mathcal{A} \subseteq \mathbb{R}^{d_a}$ as visual space and semantic space respectively, where d_x and d_a are dimensions of these two space. Then $\mathbf{x} \in \mathcal{X}$ and $\mathbf{a} \in \mathcal{A}$ represent the feature instances and their corresponding semantics (represented as column vectors). Given the training set $\mathcal{D}^s = \{\mathbf{x}, y, \mathbf{a}_y | \mathbf{x} \in \mathcal{X}, y \in \mathcal{Y}^s, \mathbf{a}_y \in \mathcal{A}\}$, the goal of ZSL is to learn a classifier towards the unseen classes: $f_{zsl} : \mathcal{X} \rightarrow \mathcal{Y}^u$, while GZSL aims to classify samples that either belongs to seen classes or unseen classes, i.e., $f_{gzsl} : \mathcal{X} \rightarrow \mathcal{Y}^s \cup \mathcal{Y}^u$. We mainly discuss the challenges in GZSL setting in this work.

3.1 Preliminary: Generative ZSL Framework Based on WGAN

In this paper, we focus on the semantic weak generalization problem in the generative-based ZSL framework. Generative-based methods decompose the ZSL

problem into two steps, i.e., the zero-shot generation and classifier training. Given the visual-semantic feature pairs, a conditional generative model is first trained. Then we use unseen semantics to generate simulated unseen samples, based on which the ZSL or GZSL classifier is then trained.

WGAN-GP [15] is a typical generator choice in existing ZSL researches, which contains a generator G and a discriminator D and optimized by the following object:

$$\mathcal{L} = \mathbb{E}_{\mathbf{x} \sim p_r} [D(\mathbf{x}, \mathbf{s})] - \mathbb{E}_{\tilde{\mathbf{x}} \sim p_g} [D(\tilde{\mathbf{x}}, \mathbf{s})] - \lambda_0 \mathbb{E}_{\hat{\mathbf{x}} \sim p_{\hat{\mathbf{x}}}} [(\nabla_{\hat{\mathbf{x}}} \|D(\hat{\mathbf{x}}, \mathbf{s})\|_2)^2 - 1], \quad (1)$$

where p_r denotes the true distribution of input visual feature, p_g denotes the distribution of generated feature, as $\tilde{\mathbf{x}} = G(\mathbf{z}_0, \mathbf{s})$, and $\hat{\mathbf{x}} = \alpha \mathbf{x} + (1 - \alpha)\tilde{\mathbf{x}}$ with $\alpha \sim U(0, 1)$ is for calculating the gradient penalty and λ_0 is a hyper-parameter.

3.2 Weakness in Semantic Generalization

Definition of Semantic Generalization. Motivated from typical supervised classification models, where we say it generalize when the conditional probability $q(y|\mathbf{x})$ learned from the empirical distribution $p(\mathbf{x}, y)$ fit well in the test set. Similarly, let p_r^s and p_r^u be the real seen and unseen distribution respectively, we have the definition:

Definition 1. *Semantic generalization in zero-shot generation is the conditional probability $p_g(\mathbf{x}|\mathbf{a}, \mathbf{z})$ modeled on $p_r^s(\mathbf{x}, \mathbf{a}|\mathbf{a} \in \mathcal{A}^s)$ well fit $p_r^u(\mathbf{x}, \mathbf{a}|\mathbf{a} \in \mathcal{A}^u)$, where $p(\mathbf{z}) = \mathcal{N}(\mathbf{0}, I)$ is the latent distribution introduced by the generative model. We define the mean class Maximum Mean Discrepancy (MMD) [2, 40] between the generated and real unseen distribution as the measurement of generalization level, which is estimated by*

$$\begin{aligned} \text{MMD}(p_g || p_r^u) &= \frac{1}{|\mathcal{Y}^u|} \sum_{y=1}^{|\mathcal{Y}^u|} \left\{ \frac{1}{n_y(n_y - 1)} \sum_{i,j=1, i \neq j}^{n_y} [\kappa(x_i^y, x_j^y) + \kappa(\tilde{x}_i^y, \tilde{x}_j^y)] \right. \\ &\quad \left. - \frac{2}{n_y^2} \sum_{i,j=1}^{n_y} \kappa(x_i^y, \tilde{x}_j^y) \right\}, \kappa(\mathbf{x}, \mathbf{x}') = 2d_x / (2d_x + \|\mathbf{x} - \mathbf{x}'\|^2), \end{aligned} \quad (2)$$

where x_i^y and \tilde{x}_i^y are samples corresponding to class y in the test unseen set and the generated unseen set, respectively, n_y is the sample number in test class y , and $\kappa(\cdot)$ is generally an arbitrary positive-definite reproducing kernel function (we employ the Inverse Multiquadratic (IM) kernel [2, 36] here). We randomly generated unseen samples with the same number as test set for each class. Generally, MMD measures the similarity between the two distributions, which is closer to 0 when the two distribution is closer, thus to effectively reflect the fitting degree of the generated distribution and the real distribution.

Empirical Analysis on Generalization Bound. In this part, we conduct a series of comparative experiments to explore the semantic generalization bound

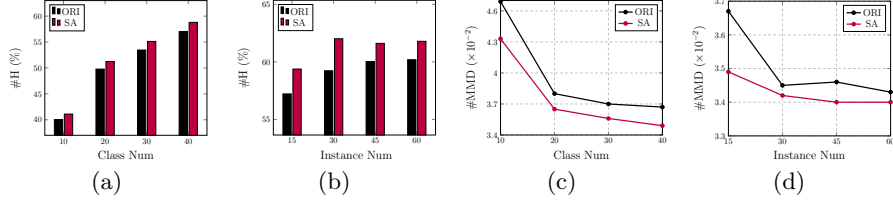


Fig. 2: Empirical analysis on the generalization bound of the original WGAN (averaged by ten random experiments on AWA2). **(a), (c)**: H score and MMD value w.r.t. the amount of classes. **(b), (d)**: H score and MMD value w.r.t. the amount of visual instance involved in training. **ORI** and **SA** denote the original and the semantic augmentation results, respectively.

in zero-shot generation. In supervised classification tasks, the diversity of the generalizing objects (e.g., images, in image classification) largely determines the generalization ability of the classifier. In analogy to the zero-shot generation task, we investigate the diversity of generalizing objects (semantics). Our study is divided into three parts. First, *(i) we maintain the amount of visual features (to reduce the impact of visual feature diversity), and randomly sample different number of classes (one category is associated with one semantic) to compare the generalization result.* Since the change in the number of classes will inevitably lead to changes in the diversity of visual features, we continued to carry out the other two experiments. On the one hand, *(ii) we maintain the number of classes unchanged, and increase the number of visual features.* On the other hand, *(iii) we keep the amount of visual features and augment the semantics in the input of the generator with Gaussian noise, which is counter-intuitive but reasonable (similar to image augmentation in other vision tasks), i.e.,*

$$G(\mathbf{z}_0, \mathbf{a}) \rightarrow G(\mathbf{z}_0, \mathbf{a} + \mathbf{z}_1), \mathbf{z}_0 \in \mathcal{N}(\mathbf{0}, \mathbf{I}), \mathbf{z}_1 \in \mathcal{N}(\mathbf{0}, \sigma \mathbf{I}). \quad (3)$$

where σ decides the standard deviation of the sampled distribution. We conduct the experiments on original WGAN [15], and the results are plotted in Fig. 2.

As shown in Fig. 2 (a), (c), when the amount of classes involved in training grows, a improved GZSL performance and a smaller MMD value can be obtained. This is in line with our expectations, because a similar conclusion that increasing the number of generalization objects can produce the generalization gains has been drawn in classification tasks. In the meanwhile, the increase of the class number brings richer visual features, alleviating the domain shift problem [12]. However, Fig. 2 (b), (d) indicate that the increase in the number of visual features quickly saturates the generalization gain, which suggest that increasing the number of visual features has a limited beneficial effect on generalization. Surprisingly, semantic augmentation yields considerable positive results in all cases, which demonstrates that merely increasing semantic diversity enhances semantic generalization, shown as the red histograms and lines in Fig. 2. This phenomenon, together with the observation of the above experiments, shows that semantic diversity is an important influencing factor of semantic generalization performance. More details are described in supplemental.

Table 1: Effects of overfitting suppression regularization methods on the generator, measured on AWA2. **ORI**: the original WGAN. **L2 Norm**: L2 regularization. **FGM**: Fast Gradient Method. **SA**: Semantic Augmentation.

Method	T1	A^u	A^s	H	MMD
ORI	68.0	57.2	70.4	63.1	0.0345
L2 Norm	71.1	59.3	72.4	65.2	0.0337
FGM	73.4	60.8	71.2	65.6	0.0333
SA	72.7	61.7	70.7	65.9	0.0335

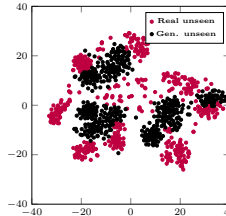


Fig. 3: t-SNE visualization of the real and generated unseen samples on AWA2, where an obvious inconsistency can be observed.

We plot the t-SNE visualization of the real and generated unseen samples in Fig. 3, which reveals a substantial bias in the generated unseen distribution. This reflects the existing technology’s weakness in semantic generalization. A strategy that can learn the real classification boundaries on biased data is also significant, in addition to improving generalization abilities. Then, in the generator (ante-hoc) and classifier (post-hoc) training stages, we illustrate the research approach for these challenges.

3.3 Ante-hoc: Semantic Generalization Strengthen

Overfitting Suppression Regularization. Sec 3.2 shows that the semantic generalization in the zero-shot generation follows the same gain pattern as feature generalization in supervised classification. Benefit from well-established research on generalization problems in supervised classification tasks, we refer to the typical overfitting suppression regularization criterion. As shown in Tab. 1, we test the performance of L2 regularization, the Fast Gradient Method [14] (an adversarial training method), and Semantic Augmentation, respectively (detailed in supplemental), which all bring improvement to the original WGAN. It is worth noting that basic semantic augmentation produce comparable results to the more complicated strategy (i.e., FGM). We experimentally analyze the effective mechanism of semantic augmentation in Sec. 4.1, which is proved to construct latent semantic-visual relationships. In subsequent experiments, we will augment the semantic input of the generator as Eq. 3 (no additional operations are performed on the discriminator).

Fitting Target Relaxation. [37] has shown that the generation quality of GAN decreases as the complexity of the dataset increases. Intuitively, we can remove the redundant information from the visual features to reduce the fitting pressure on the generator, in other words, to fit only the key information. Generally, the classifier in generative-based ZSL is composed of a linear softmax network. In this paper, we use the cosine similarity to calculate the similarity between input feature and the weight row vectors instead of the dot product, which is

known as leaning the class prototypes in existing researches [27,48,29,39]. In this circumstance, the scale information is redundant for instances, because the scale is normalized in calculating cosine distance. Naturally, we remove the scale information in the GAN training, resulting in 1 degree of freedom relaxation of the fitting target:

$$\mathbf{x} := \frac{\mathbf{x}}{\|\mathbf{x}\|_2}, \quad (4)$$

where $\|\cdot\|_2$ denotes the l_2 norm.

3.4 Post-hoc: Classifier Training with Partially Biased Data

Since the intractable of the semantic weak generalization problem, we focus another part of our attention on designing a correct classifier optimization direction with biased data to obtain better classification results on real test data. Then how can we design the optimization direction? Let us observe the three kind of decision boundaries in GZSL, i.e., the decision boundaries between different seen classes, between different unseen classes, and between seen and unseen classes. For the first boundaries, optimizing on the empirical distribution is generally enough to produce satisfactory effect. On the contrary, it is difficult to find a clear guidance for the second boundaries, due to the unpredictability of data bias. Moreover, for the third boundaries, the phenomenon of seen-unseen bias can be a direct optimization Guideline. Hence, we design the training objective of the classifier with two principles: (1) mitigating the impact of biased samples (simulated unseen samples) on decision bounds between different real samples (seen samples) during training, and (2) reducing the seen-unseen bias.

Base Classifier. Suppose we have obtained a batch of simulated unseen samples from the trained generator, and define the linear classifier $f_c(\cdot)$ with weight parameters $\mathbf{W} \in \mathbb{R}^{|\mathcal{Y}| \times d_x}$. With slightly abuse of notation, we subsequently use \mathbf{x} to denote both the real and generated data, and use the original notation for the normalized results, i.e., $\mathbf{W}_y := \frac{\mathbf{W}_y}{\|\mathbf{W}_y\|_2}$ and $\mathbf{x} := \frac{\mathbf{x}}{\|\mathbf{x}\|_2}$ for the convenient expression of cosine similarity, where the subscript y denotes the y -th row in \mathbf{W} . Then we optimize the classifier with cross-entropy:

$$f_c(\mathbf{x}) = \mathbf{W} \cdot \mathbf{x}, \mathcal{L}_{ce} = \sum_i -\log \frac{\exp(\mathbf{W}_{y_{x_i}} \cdot \mathbf{x}_i / \tau)}{\sum_{y \in \mathcal{Y}^s \cup \mathcal{Y}^u} \exp(\mathbf{W}_y \cdot \mathbf{x}_i / \tau)}, \quad (5)$$

where τ is the temperature [19].

Principle Guided Classifier Revision. Towards the principle (1), we first represent the change brought by the newly added unseen class as the incremental form of the loss function on the original seen class, i.e.,

$$\begin{aligned} \mathcal{L}_{ce} = & \sum_{y_{x_i} \in \mathcal{Y}^s} -\log \frac{\exp(\mathbf{W}_{y_{x_i}} \cdot \mathbf{x}_i / \tau)}{\sum_{y \in \mathcal{Y}^s} \exp(\mathbf{W}_y \cdot \mathbf{x}_i / \tau) + \lambda_1 \sum_{y \in \mathcal{Y}^u} \exp(\mathbf{W}_y \cdot \mathbf{x}_i / \tau)} \\ & + \lambda_2 \sum_{y_{x_i} \in \mathcal{Y}^u} -\log \frac{\exp(\mathbf{W}_{y_{x_i}} \cdot \mathbf{x}_i / \tau)}{\sum_{y \in \mathcal{Y}^s \cup \mathcal{Y}^u} \exp(\mathbf{W}_y \cdot \mathbf{x}_i / \tau)}, \end{aligned} \quad (6)$$

where we introduce the parameters λ_1 and λ_2 for the generalized incremental forms. It is obvious that biased unseen samples will have little effect on the decision boundaries between seen classes when λ_1 and λ_2 is close to 0. Then we calculate the gradient of the unseen class weight:

$$\begin{aligned} \frac{\partial \mathcal{L}_{ce}}{\partial \mathbf{W}_u} = & \sum_{y_{\mathbf{x}_i} \in \mathcal{Y}^s} \frac{\lambda_1 \exp(\mathbf{W}_{y_{\mathbf{x}_i}} \cdot \mathbf{x}_i) \cdot \mathbf{x}_i^T / \tau}{\sum_{y \in \mathcal{Y}^s} \exp(\mathbf{W}_y \cdot \mathbf{x}_i / \tau) + \lambda_1 \sum_{y \in \mathcal{Y}^u} \exp(\mathbf{W}_y \cdot \mathbf{x}_i / \tau)} \\ & - \lambda_2 \left[\sum_{y_{\mathbf{x}_i} = u} \mathbf{x}_i^T / \tau - \sum_{y_{\mathbf{x}_i} \in \mathcal{Y}^u} \frac{\exp(\mathbf{W}_u \cdot \mathbf{x}_i) \cdot \mathbf{x}_i^T / \tau}{\sum_{y \in \mathcal{Y}^s \cup \mathcal{Y}^u} \exp(\mathbf{W}_y \cdot \mathbf{x}_i / \tau)} \right]. \end{aligned} \quad (7)$$

Assume a decomposition of \mathbf{x} , i.e., $\mathbf{x} = \mathbf{x}^c + \mathbf{x}^i$, where \mathbf{x}^c contains the common information for all data and \mathbf{x}^i contains the independent information of \mathbf{x} (which is a reasonable decomposition due to the redundancy of the data [38]). Due to the gradient descent optimization, the first item in Eq. 7 makes $\mathbf{W}_u \cdot \mathbf{x}^c$ smaller while the second item makes $\mathbf{W}_u \cdot \mathbf{x}^c$ bigger. This means a smaller λ_1 and a bigger λ_2 make the \mathbf{x} in the data distribution to have a greater probability of being predicted as class u , which provide a direction to mitigate the seen-unseen bias, i.e., principle (2). See supplementary material for the detailed derivation.

In summary, a small λ_1 and a suitable λ_2 fit the two principle, which guides a classifier revision direction. Specifically, we remove a part of the terms corresponding to the weight of the unseen class in the denominator term of the first item in Eq. 7, and remove the parameter λ_2 since it has the same optimization direction as the synthetic number of unseen classes. Then we have the revised cross-entropy, i.e.,

$$\begin{aligned} \mathcal{L}_{rce} = & \sum_{y_{\mathbf{x}_i} \in \mathcal{Y}^s} -\log \frac{\exp(\mathbf{W}_{y_{\mathbf{x}_i}} \cdot \mathbf{x}_i / \tau)}{\sum_{y \in \mathcal{Y}^s} \exp(\mathbf{W}_y \cdot \mathbf{x}_i / \tau) + \lambda_1 \sum_{j=u_1}^{u_k} \exp(\mathbf{W}_{y_j} \cdot \mathbf{x}_i / \tau)} \\ & + \sum_{y_{\mathbf{x}_i} \in \mathcal{Y}^u} -\log \frac{\exp(\mathbf{W}_{y_{\mathbf{x}_i}} \cdot \mathbf{x}_i / \tau)}{\sum_{y \in \mathcal{Y}^s \cup \mathcal{Y}^u} \exp(\mathbf{W}_y \cdot \mathbf{x}_i / \tau)}, \end{aligned} \quad (8)$$

where $\{u_i\}_{i=1}^k = \arg \text{top}_k \{\mathbf{W}_{y_j} \cdot \mathbf{x} \mid y_j \in \mathcal{Y}^u\}$.

Intuitively, the top k selection create a concentration on the hard class and also in line with the previous guidelines. Based on Eq. 7, when λ_1 is small enough, a seen datum can focus on the decision boundary with other seen classes during training, through which the compromises made to stay away from biased unseen domains is mitigated. As shown in Fig. 4 (c), (d), the classifier obtained with a suitable value of λ_1 has stronger discriminability between seen classes, and has a smaller seen-unseen bias.

Bound Classification Weights with Semantics. Semantics in ZSL contain the key discriminant information, which is especially important for unseen classes. We directly employ a mapping network $M(\cdot)$ to map semantics to classification weights to overcome the previous drawback of constraining weights by

visual relations only, i.e.,

$$\mathbf{W}_y = M(\mathbf{a}_y), y \in \mathcal{Y}^s \cup \mathcal{Y}^u, \quad (9)$$

which replaces the weights in Eq. 8.

3.5 Inference

In inference, a datum \mathbf{x} is predicted in the class corresponding to the weight with the largest cosine similarity from \mathbf{x} , i.e.,

$$\hat{y} = \arg \max_i \mathbf{W}_i \cdot \mathbf{x}, \quad (10)$$

where needs to be emphasized that \mathbf{x} and \mathbf{W}_i are notations after normalization.

4 Experiments

4.1 Toy Experiment: Why Semantic Augmentation Effective

Despite the effectiveness of the semantic augmentation (SA) approach, we further conduct a toy experiment to illustrate its action mode.

Setup. We consider a 2-D dataset sampled from Unit Gaussian distribution, i.e., $\mathcal{D}^{toy} = \{\mathbf{x}_i\}, \mathbf{x}_i \in \mathcal{N}(\mathbf{0}, \mathbf{I})$. We define the coordinates on the 2-D plane as the semantics, a semantic defines a Gaussian distribution centered on it. We only attach to 1 semantic in this case, i.e., $\mathbf{a} = [0, 0]$. The toy data are plotted in Fig. 4 (a). Then we sample the noise \mathbf{z} from an additional prior distribution $\mathcal{N}(\mathbf{0}, \mathbf{I})$ to concatenate with \mathbf{a} and train WGAN.

Toy Experiment Analysis. After training, we fix \mathbf{z} to $[0, 0]$ and sample different \mathbf{a} from $\mathcal{N}(\mathbf{0}, \mathbf{I})$ to show the generation results. According to our definition, the semantic reflects the position on the 2-D plane. However, the synthesized result without SA in Fig. 4 (b) shrinks to a small range. This is because the model trained with a single semantic can not attach to this information. In contrast, the SA result in Fig. 4 (c) shows a Gaussian distribution. According to our preset, the sample points in the dataset can be considered to be defined in different semantics. When augmenting the semantic in the input of the generator with a small variance Gaussian noise, the samples generated by the augmented semantics are constrained to the groundtruth space by optimization, through which the small variance of semantics automatically correspond to locations in visual space, just as generative models enable additional prior noise to be regularly mapped into the feature space. A anomalous distribution is observed in Fig. 4 (d), which is trained by SA with large variance noises. Intuitively, the feature generated with large variance semantics creates a high probability of being outside the groundtruth domain, which also breaks the rules of the setup.

Real Scenario Analysis. Assuming that semantic descriptors describe all important visual features, ideally, a semantic descriptor can uniquely identify a location in the visual space. However, we can only obtain the collective description of each class in ZSL setting. The generative network only learns the positional differences of large semantic gaps (i.e., semantics of different categories) in

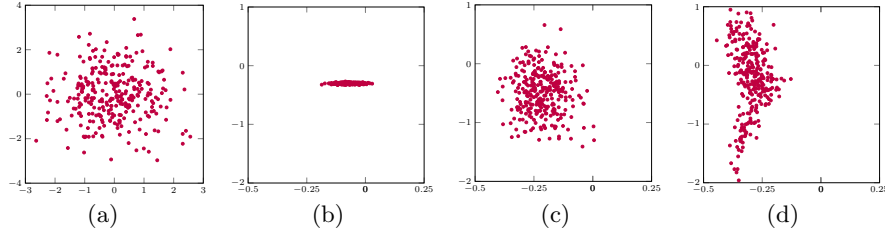


Fig. 4: Illustration of the toy experiment in Sec. 4.1. (a) 2-D groundtruth sampled from the Unit Gaussian distribution. (b) (c) WGAN generated samples without or with semantic augmentation during training. (d) Semantic augmentation with large variance.

the visual space, unable to capture the response of small semantic changes. By augmenting semantics with small variance noises, and constraining the generated visual features within their corresponding categories through optimization, small semantic changes find the direction of change in the visual space. As a result, the generator learns additional implicit semantic-visual relations, which act as an inductive bias to improve its generalization ability on unseen semantics.

4.2 Real Data Experimental Settings

Benchmark Datasets. We conduct GZSL experiments on four popular ZSL datasets. Animals with Attributes 2 (AWA2) [25] contains 50 animal species and 85 attribute annotations, accounting 37,322 samples. Attribute Pascal and Yahoo (APY) [9] includes 32 classes of 15,339 samples and 64 attributes. Caltech-UCSD Birds-200-2011 (CUB) [43] consists of 11,788 samples with 200 bird species, annotated by 312 attributes. SUN Attribute (SUN) [34] carries 14,340 images from 717 different scenario-style with 102 attributes. We then split the data into seen and unseen classes according to the benchmark procedure in [45].

Representation. For visual representations, we follow [45] to represent the image as the 2048-dimensional visual features, which is extracted from the pre-trained ResNet101 [18] without fine-tuning on seen data. For class representations (i.e., semantics), we regard the artificial attribute annotations of datasets as the semantic descriptors of AWA2, APY, and SUN, and come the 1024-dimensional character-based CNN-RNN features [35] generated from textual descriptions as the semantics of CUB, for a fair comparison with SoTAs.

Evaluation Metric. We calculate the average per-class top-1 accuracy on the unseen and seen classes respectively, denoted as A^u and A^s , then their harmonic mean H is employed as the measurement of GZSL. The classic ZSL is evaluated with per-class averaged top-1 accuracy on unseen classes [45].

4.3 Implementation Details

The Generator G is implemented by multi-layer perceptron (MLP) with two hidden layers of 4096 and 2048 dimensions. The Discriminator contains one 4096-D hidden layer, and the mapping net M includes a 1024-D hidden layer. All the

Table 2: GZSL performance of ours and the state-of-the-art methods on four popular benchmarks, where \dagger and \S denote the non-generative and generative methods, respectively. A^u and A^s represent per-class accuracy scores (%) on seen and unseen test samples, and H is their harmonic mean. The best result is bolded.

Method	Source	AWA2			CUB			SUN			APY		
		A^u	A^s	H	A^u	A^s	H	A^u	A^s	H	A^u	A^s	H
Li et al. [27]	ICCV' 19	56.4	81.4	66.7	47.4	47.6	47.5	36.3	42.8	39.3	26.5	74.0	39.0
TCN [21]	ICCV' 19	61.2	65.8	63.4	52.6	52.0	52.3	31.2	37.3	34.0	24.1	64.0	35.1
\dagger APNet [30]	AAAI' 20	54.8	83.9	66.4	48.1	55.9	51.7	35.4	40.6	37.8	32.7	74.7	45.5
CN-GZSL [39]	ICLR' 21	60.2	77.1	67.6	49.9	50.7	50.3	44.7	41.6	43.1	-	-	-
IPN [29]	ICLR' 21	67.5	79.2	72.9	60.2	73.8	66.3	-	-	-	37.2	66.0	47.6
f-CLSWGAN [44]	CVPR' 18	-	-	-	43.7	57.7	49.7	42.6	36.6	39.4	-	-	-
TF-VAEGAN [32]	ECCV' 20	59.8	75.1	66.6	52.8	64.7	58.1	45.6	40.7	43.0	-	-	-
LsrGAN [42]	ECCV' 20	54.6	74.6	63.0	48.1	59.1	53.0	44.8	37.7	40.9	-	-	-
Chou et al. [7]	ICLR' 21	65.1	78.9	71.3	41.4	49.7	45.2	29.9	40.2	34.3	35.1	65.5	45.7
GCM-CF [49]	CVPR' 21	60.4	75.1	67.0	61.0	59.7	60.3	47.9	37.8	42.2	37.1	56.8	44.9
\S CE-GZSL [16]	CVPR' 21	63.1	78.6	70.0	63.9	66.8	65.3	48.8	38.6	43.1	-	-	-
FREE [4]	ICCV' 21	60.4	75.4	67.1	55.7	59.9	57.7	47.4	37.2	41.7	-	-	-
SDGZSL [6]	ICCV' 21	64.6	73.6	68.8	59.9	66.4	63.0	-	-	-	38.0	57.4	45.7
HSVA [5]	NeurIPS' 21	56.7	79.8	66.3	52.7	58.3	55.3	-	-	-	-	-	-
TSWG	Proposed	67.4	81.0	73.6	70.1	68.3	69.2	48.6	39.4	43.5	38.6	67.2	49.1

hidden layers are activated by Leaky-ReLU. We follow [44] to set other hyperparameters in WGAN. In addition, we set 512 for the (mini) batch size, and adopt Adam [22] as the optimizer of all the nets with learning rate of 1.0×10^{-4} .

4.4 Comparison with State-of-the-Arts

The GZSL comparison results are shown in Tab. 2. We report the official results of the state-of-the-art methods from referenced articles with the identical experimental setting used in this paper for fair comparison. It can be observed that our results outperform the SoTAs in all of the four datasets. This is mostly due to the ant-hoc and post-hoc strategies jointly balance the accuracy of seen and unseen classes, from which a significant higher unseen accuracy can be obtained. The accuracy in AWA2, CUB and APY are particularly higher than others. Since the coarse-grained or slightly fine-grained datasets have a small semantic diversities, which means a more severe biased generated unseen distribution, our straight-through semantic generalization and learning-on-biased-data schemes yield greater gains. In contrary, the result has fewer advantages in the extremely fine-grained SUN dataset due to its richer number of classes and semantics.

4.5 Ablation Study

Baselines. We conduct an ablation study to validate the effect of each component, including the ante-hoc and post-hoc operations on AWA2 and CUB datasets. The following Baselines are proposed. (i) We set σ to 0 in the full model. (ii) The generator fits the visual features before normalization. (iii) Do

Table 3: Ablation study results of GZSL Table 4: Discriminability on unseen on AWA2 and CUB. The baselines are classes, evaluated by ZSL performance (%) (comparison with SoTAs). constructed by removing some key modules. **SA**: Semantic Augmentation; **TR**: Target Relaxation; **CR**: Classifier Revision; **M**: Mapping Net. **Note** that our classifier is obtained with targeting at GZSL.

Ablation	AWA2			CUB		
	A^u	A^s	H	A^u	A^s	H
(i) SA	66.4	77.2	71.4	72.2	66.1	69.0
Ante (ii) TR	66.7	80.0	72.7	70.8	67.1	68.9
(iii) SA&TR	65.9	77.7	71.3	72.1	65.8	68.8
(iv) CR	39.8	89.4	55.1	58.3	70.9	64.0
Post (v) M	64.0	79.4	70.9	70.7	57.8	63.6
(vi) CR&M	34.7	90.0	50.0	44.7	70.2	54.7
Full Model	67.4	81.0	73.6	70.1	68.3	69.2

Method	AWA2	CUB	SUN	APY
TCN [21]	71.2	59.5	61.5	38.9
LisGAN [26]	-	58.8	61.7	43.1
TF-VAEGAN [32]	72.2	64.9	66.0	-
Chou et al. [7]	73.8	57.2	63.3	41.0
IPN [29]	74.4	59.6	-	42.3
CE-GZSL [16]	70.4	77.5	63.3	-
SDGZSL [6]	72.1	75.5	-	45.4
TSWG	74.0	80.1	65.4	46.6

(i) and (ii) operations at the same time. (iv) Train the classifier with revision, i.e., with Eq. 5. (v) Without mapping net, i.e., optimizing the randomly generated weights. (vi) Do (iv) and (v) operations at the same time.

Results. The above-mentioned baselines are compared in Tab. 3 with the GZSL performance. Through our test, **Baseline i, ii, iii** show that the ante-hoc process produces fewer effects on the fine-grained dataset CUB than on the coarse-grained dataset AWA2, mainly because of the inherently small data biased caused by more types of semantics in generator training in the CUB (40 in AWA2 vs 150 in CUB). Meanwhile, for the same reason, classifier revision plays a bigger role for AWA2 than CUB (Baseline iv). The mapping net is more important for CUB, as shown in Baseline v. Since the difficulty of discriminating fine-grained visual features, the classifier weights from the mapping net utilize semantic prior information, which is of great help for fine-grained discrimination. Overall, due to the difficulty of solving the problem of weak semantic generalization, post-hoc process brings more considerable benefits than ante-hoc process.

4.6 Hyper-parameters

There are mainly five hyper-parameters that control the objective function, i.e., σ , τ , k , λ_1 , and the generated number per unseen class. For τ , we follow [39] to assign it a value of 0.04 on all datasets. Due to the consistent optimization direction of k and λ_1 , we dynamically set k to 1 when a seen datum is predicted to one of the unseen class, and 0 otherwise. Then we empirically analyze the influence of other three parameters. As shown in Fig. 5 (b), A^u and H have the same trend when σ varies, which demonstrates its ability to control the semantic generalization effect. A big σ lead to performance degradation, because a large variance of noise intuitively makes the semantic input of the generator lose inter-class discriminability. A small λ_1 mitigates the seen-unseen bias in Fig. 5 (c). In the meanwhile, a suitable generated number create the best performance, as shown in Fig. 5 (a), and the number is much smaller than the existing generative

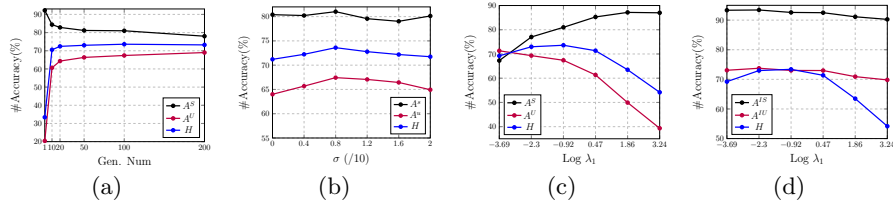


Fig. 5: (a), (b), (c) GZSL effects w.r.t. the generated number for each unseen classes, σ , and λ_1 . (d) Intra-discriminability of seen and unseen classes w.r.t. λ_1 , where A^{is} and A^{iu} represent the intra- seen or unseen classes accuracy, and H is still the harmonic mean of A^s and A^u . We conduct the study on AWA2.

based methods (100 vs 2400 in [16] and 4600 in [4]). This demonstrates the joint effect of the number of generations and λ_1 we stated in Sec. 3.4. We also report the effect of λ_1 on the discriminability of intra-seen classes in Fig. 5 (d), which shows a downward trend when λ_1 increases within a certain range. We empirically generate 50 samples per unseen class in CUB, SUN, and APY, and 100 for AWA2 in the experiment. We set σ to 0.08 and λ_1 to 12, 0.4, 1 and 0.4, respectively, for the best results.

4.7 Discriminability on Unseen Classes

We intuitively analyze the discriminability of the trained classifier on unseen classes, which is obtained under the GZSL setting. We directly employ the ZSL accuracy as the measurement, compared with the SoTA methods in Tab. 4. Surprisingly, although our model does not target ZSL directly, it still achieves promising ZSL performance, even comparable to SoTA methods trained towards ZSL setting. We believe that there are two main reasons for the good discriminability on unseen classes, one is the improvement of semantic generalization ability by ante-hoc processing, and the other is the inductive bias of the classifier weights derived from semantic mapping.

5 Conclusions

In this paper, we propose the semantic weak generalization problem in generative-based Zero-Shot Learning, and design a simple and effective method with its guidance. We investigate methods for enhancing semantic generalization and learning correct decision boundaries with biased data, respectively. The proposed method does not produce additional resource consumption compared to the vanilla WGAN based Zero-Shot method, but outperforms SoTAs by a large margin. Beyond the performance improvement brought by our simple method, we think the formulation of the semantic generalization problem has a greater role in guiding future research. In the future, we will dig deeper to enhance semantic generalization and reduce the bias between the generated and the ground-truth unseen class distributions in generative ZSL.

References

1. Akata, Z., Perronnin, F., Harchaoui, Z., Schmid, C.: Label-embedding for attribute-based classification. In: CVPR. pp. 819–826 (2013)
2. Ardizzone, L., Kruse, J., Wirkert, S., Rahner, D., Pellegrini, E.W., Klessen, R.S., Maier-Hein, L., Rother, C., Köthe, U.: Analyzing inverse problems with invertible neural networks. ICLR (2018)
3. Chao, W.L., Changpinyo, S., Gong, B., Sha, F.: An empirical study and analysis of generalized zero-shot learning for object recognition in the wild. In: ECCV. pp. 52–68 (2016)
4. Chen, S., Wang, W., Xia, B., Peng, Q., You, X., Zheng, F., Shao, L.: Free: Feature refinement for generalized zero-shot learning. ICCV (2021)
5. Chen, S., Xie, G., Liu, Y., Peng, Q., Sun, B., Li, H., You, X., Shao, L.: Hsua: Hierarchical semantic-visual adaptation for zero-shot learning. NeurIPS **34** (2021)
6. Chen, Z., Luo, Y., Qiu, R., Huang, Z., Li, J., Zhang, Z.: Semantics disentangling for generalized zero-shot learning. In: ICCV (2021)
7. Chou, Y.Y., Lin, H.T., Liu, T.L.: Adaptive and generative zero-shot learning. In: ICLR (2021)
8. Dinu, G., Lazaridou, A., Baroni, M.: Improving zero-shot learning by mitigating the hubness problem. ICLR work shop (2014)
9. Farhadi, A., Endres, I., Hoiem, D., Forsyth, D.: Describing objects by their attributes. In: CVPR. pp. 1778–1785 (2009)
10. Felix, R., Reid, I., Carneiro, G., et al.: Multi-modal cycle-consistent generalized zero-shot learning. In: ECCV. pp. 21–37 (2018)
11. Frome, A., Corrado, G., Shlens, J., Bengio, S., Dean, J., Ranzato, M., Mikolov, T.: Devise: A deep visual-semantic embedding model. NeurIPS p. 2121–2129 (2013)
12. Fu, Y., Hospedales, T.M., Xiang, T., Fu, Z., Gong, S.: Transductive multi-view embedding for zero-shot recognition and annotation. In: ECCV. pp. 584–599. Springer (2014)
13. Goodfellow, I., Pouget-Abadie, J., Mirza, M., Xu, B., Warde-Farley, D., Ozair, S., Courville, A., Bengio, Y.: Generative adversarial nets. NeurIPS **27** (2014)
14. Goodfellow, I.J., Shlens, J., Szegedy, C.: Explaining and harnessing adversarial examples. arXiv preprint arXiv:1412.6572 (2014)
15. Gulrajani, I., Ahmed, F., Arjovsky, M., Dumoulin, V., Courville, A.: Improved training of wasserstein gans. arXiv preprint arXiv:1704.00028 (2017)
16. Han, Z., Fu, Z., Chen, S., Yang, J.: Contrastive embedding for generalized zero-shot learning. In: CVPR. pp. 2371–2381 (2021)
17. Han, Z., Fu, Z., Yang, J.: Learning the redundancy-free features for generalized zero-shot object recognition. In: CVPR. pp. 12865–12874 (2020)
18. He, K., Zhang, X., Ren, S., Sun, J.: Deep residual learning for image recognition. In: CVPR. pp. 770–778 (2016)
19. Hinton, G., Vinyals, O., Dean, J.: Distilling the knowledge in a neural network. NeurIPS (2015)
20. Huynh, D., Elhamifar, E.: Fine-grained generalized zero-shot learning via dense attribute-based attention. In: CVPR. pp. 4483–4493 (2020)
21. Jiang, H., Wang, R., Shan, S., Chen, X.: Transferable contrastive network for generalized zero-shot learning. In: ICCV. pp. 9765–9774 (2019)
22. Kingma, D.P., Ba, J.: Adam: A method for stochastic optimization. ICLR (2015)
23. Kingma, D.P., Welling, M.: Auto-encoding variational bayes. ICLR (2013)

24. Lampert, C.H., Nickisch, H., Harmeling, S.: Learning to detect unseen object classes by between-class attribute transfer. In: CVPR. pp. 951–958 (2009)
25. Lampert, C.H., Nickisch, H., Harmeling, S.: Attribute-based classification for zero-shot visual object categorization. *IEEE TPAMI* **36**(3), 453–465 (2013)
26. Li, J., Jing, M., Lu, K., Ding, Z., Zhu, L., Huang, Z.: Leveraging the invariant side of generative zero-shot learning. In: CVPR. pp. 7402–7411 (2019)
27. Li, K., Min, M.R., Fu, Y.: Rethinking zero-shot learning: A conditional visual classification perspective. In: ICCV. pp. 3583–3592 (2019)
28. Li, Y., Wang, D., Hu, H., Lin, Y., Zhuang, Y.: Zero-shot recognition using dual visual-semantic mapping paths. In: CVPR. pp. 3279–3287 (2017)
29. Liu, L., Zhou, T., Long, G., Jiang, J., Dong, X., Zhang, C.: Isometric propagation network for generalized zero-shot learning. *ICLR* (2021)
30. Liu, L., Zhou, T., Long, G., Jiang, J., Zhang, C.: Attribute propagation network for graph zero-shot learning. In: *AAAI*. vol. 34, pp. 4868–4875 (2020)
31. Mikolov, T., Chen, K., Corrado, G., Dean, J.: Efficient estimation of word representations in vector space. *ICLR Work-shop Papers* (2013)
32. Narayan, S., Gupta, A., Khan, F.S., Snoek, C.G., Shao, L.: Latent embedding feedback and discriminative features for zero-shot classification. In: *ECCV*. pp. 479–495 (2020)
33. Palatucci, M.M., Pomerleau, D.A., Hinton, G.E., Mitchell, T.: Zero-shot learning with semantic output codes (2009)
34. Patterson, G., Hays, J.: Sun attribute database: Discovering, annotating, and recognizing scene attributes. In: CVPR. pp. 2751–2758 (2012)
35. Reed, S., Akata, Z., Lee, H., Schiele, B.: Learning deep representations of fine-grained visual descriptions. In: CVPR. pp. 49–58 (2016)
36. Shen, Y., Qin, J., Huang, L., Liu, L., Zhu, F., Shao, L.: Invertible zero-shot recognition flows. In: *ECCV*. pp. 614–631 (2020)
37. Shmelkov, K., Schmid, C., Alahari, K.: How good is my gan? In: *ECCV*. pp. 213–229 (2018)
38. Shwartz-Ziv, R., Tishby, N.: Opening the black box of deep neural networks via information. *arXiv preprint arXiv:1703.00810* (2017)
39. Skorokhodov, I., Elhoseiny, M.: Class normalization for (continual)? generalized zero-shot learning. *ICLR* (2021)
40. Tolstikhin, I., Bousquet, O., Gelly, S., Schoelkopf, B.: Wasserstein auto-encoders. *ICLR* (2017)
41. Verma, V.K., Brahma, D., Rai, P.: Meta-learning for generalized zero-shot learning. In: *AAAI*. vol. 34, pp. 6062–6069 (2020)
42. Vyas, M.R., Venkateswara, H., Panchanathan, S.: Leveraging seen and unseen semantic relationships for generative zero-shot learning. In: *ECCV*. pp. 70–86. Springer (2020)
43. Wah, C., Branson, S., Welinder, P., Perona, P., Belongie, S.: The caltech-ucsd birds-200-2011 dataset. *california institute of technology* (2011)
44. Xian, Y., Lorenz, T., Schiele, B., Akata, Z.: Feature generating networks for zero-shot learning. In: CVPR. pp. 5542–5551 (2018)
45. Xian, Y., Schiele, B., Akata, Z.: Zero-shot learning-the good, the bad and the ugly. In: CVPR. pp. 4582–4591 (2017)
46. Xian, Y., Sharma, S., Schiele, B., Akata, Z.: f-gan-d2: A feature generating framework for any-shot learning. In: CVPR. pp. 10275–10284 (2019)
47. Xu, W., Xian, Y., Wang, J., Schiele, B., Akata, Z.: Attribute prototype network for zero-shot learning. *NeurIPS* **33**, 21969–21980 (2020)

48. Yu, Y., Ji, Z., Han, J., Zhang, Z.: Episode-based prototype generating network for zero-shot learning. In: CVPR. pp. 14035–14044 (2020)
49. Yue, Z., Wang, T., Sun, Q., Hua, X.S., Zhang, H.: Counterfactual zero-shot and open-set visual recognition. In: CVPR. pp. 15404–15414 (2021)
50. Zhu, Y., Xie, J., Tang, Z., Peng, X., Elgammal, A.: Semantic-guided multi-attention localization for zero-shot learning. NeurIPS **32** (2019)